Published in final edited form as:
Dalton Trans. 2009 January 21; (3): 424–433. doi:10.1039/b810895a.

NMR spectroscopy and molecular modelling studies of nitrosylcobalamin: further evidence that the deprotonated, base-off form is important for nitrosylcobalamin in solution†

Hanaa A. Hassanin[a], **Luciana Hannibal**[a,b,c], **Donald W. Jacobsen**[b,c,d], **Kenneth L. Brown**[e], **Helder M. Marques**[f], and **Nicola E. Brasch**[a,b]

[a] Department of Chemistry, School of Biomedical Sciences, Kent State University, Kent, OH44242

[b] School of Biomedical Sciences, Kent State University, Kent, OH 44242. E-mail: nbrasch@kent.edu

[c] Department of Cell Biology, Lerner Research Institute, Cleveland Clinic, Cleveland, OH 44195

[d] Department of Molecular Medicine, Cleveland Clinic Lerner College of Medicine, Case Western Reserve University, Cleveland, OH 44106

[e] Department of Chemistry and Biochemistry, Ohio University, Athens, OH 45701

[f] Molecular Sciences Institute, School of Chemistry, University of the Witwatersrand, PO Wits, Johannesburg, 2050, South Africa. E-mail: Helder.Marques@wits.ac.za

Abstract

The structure of nitrosylcobalamin (NOCbl) in solution has been studied by NMR spectroscopy and the ^{1}H and ^{13}C NMR spectra have been assigned. ^{13}C and ^{31}P NMR chemical shifts, the UV-vis spectrum of NOCbl and the observed p$K_{\text{base-off}}$ value of ~5.1 for NOCbl provide evidence that a significant fraction of NOCbl is present in the base-off, 5,6-dimethylbenzimidazole (DMB) deprotonated, form in solution. NOE-restrained molecular mechanics modelling of base-on NOCbl gave annealed structures with minor conformational differences in the flexible side chains and the nucleotide loop position compared with the X-ray structure. A molecular dynamics simulation at 300 K showed that DMB remains in close proximity to the α face of the corrin in the base-off form of NOCbl. Simulated annealing calculations produced two major conformations of base-off NOCbl. In the first, the DMB is perpendicular to the corrin and its B3 nitrogen is about 3.1 Å away from and pointing directly at the metal ion; in the second the DMB is parallel to and tucked beneath the D ring of the corrin.

Introduction

Two vitamin B_{12}-dependent enzyme reactions occur in mammals – methylcobalamin-dependent methionine synthase and adenosylcobalamin-dependent L-methylmalonyl-CoA mutase.[1] The early stages of B_{12} deficiency in humans lead to hyperhomocysteinaemia and/or methylmalonic acidaemia followed by megaloblastic anaemia and/or neurological disorders.[2] The nitric oxide (NO) derivative of vitamin B_{12}, nitrosylcobalamin (NOCbl, also referred to as nitroxylcobalamin or nitrosocobalamin in the literature), is also of potential interest in mammalian biochemistry. It has recently been proposed that cobalamins (Cbls, vitamin B_{12} derivatives) scavenge nitric oxide to form NOCbl *in vivo*,[3,4] and that Cbl is beneficial in treating

†Electronic supplementary information (ESI) available: Table S1–S3 and Fig. S1. See DOI: 10.1039/b810895a

Correspondence to: Helder M. Marques; Nicola E. Brasch.

pathological disorders associated with high NO, including sepsis.[4,5] NO regulates vasodilation, neurotransmission, and the immune response and is an inhibitor of platelet aggregation and cell proliferation.[6,7] Aquacobalamin suppresses NO-induced relaxation of smooth muscle,[8–10] NO-induced vasodilation[11] and NO-mediated inhibition of cell proliferation.[3] Vitamin B_{12} (cyanocobalamin) also reverses NO-induced neural tube defects.[12] Furthermore, both MeCbl-dependent methionine synthase and adenosylcobalamin-dependent methylmalonyl-CoA mutase are inhibited by NO or NO donors.[13–17]

The extremely air sensitive NOCbl can be prepared by bubbling NO(g) through anaerobic solutions of cob(II)alamin or glutathionylcobalamin, by photoreduction of an aquacobalamin (H_2OCbl^+) solution in the presence of NO(g) using a laser, or reacting aquacobalamin with NO donors.[18–23] There has been some controversy in the literature concerning whether H_2OCbl^+ reacts directly with NO to form NOCbl, although it is now generally accepted that this is not the case.[22,24] There has also been controversy as to whether H_2OCbl^+ reacts directly with NO to form NOCbl in acidic solution (pH < 4); however commercial NO(g) is contaminated with nitrogen dioxide which reacts with NO to ultimately produce NO^+ and nitrite in aqueous solution,[24] and a recent study provides convincing evidence that the initial reaction step instead involves the formation of base-off NO_2Cbl.[25]

NOCbl has been characterized in solution by UV-vis, ^1H NMR (aromatic region only) and ^{15}N NMR spectroscopy.[18,19,23] Although the ν(N–O) stretch of NOCbl was not observed in solution by resonance Raman spectroscopy, a Co–N(O) band was observed at 514 cm^{-1}.[19] Recently some of us determined the structure of NOCbl·15H_2O by X-ray diffraction.[23] On the basis of the Co–N–O angle (117.4–121.4°) it was concluded that the oxidation state of the Co centre in NOCbl is +3 in the solid state, since the Co–N–O group of low spin NO^-–Co^{III} complexes is bent (~120°) as a consequence of the lone pair on the N atom of NO^-,[26] whereas Co–N–O is essentially linear for Co^{II}–NO complexes.[26] A similar conclusion was reached for NOCbl in solution based on resonance Raman spectroscopy measurements, the observation of well defined ^1H and ^{15}N NMR resonances indicative of a diamagnetic complex and the ^{15}N NMR chemical shift of ^{15}NOCbl.[18,19]

Some of us have previously successfully applied a molecular mechanics (MM) force field to address a variety of questions in the structural chemistry of corrins.[27–31] We have also used NMR-derived distance restraints in molecular dynamics (MD) and simulated annealing (SA) calculations to explore the solution structure of a number of corrins, including those that fail to crystallize.[32–37] In the present work we have investigated the structure of NOCbl in solution using 2-D NMR spectroscopy techniques combined with NOE-restrained molecular dynamics calculations. The ^1H and ^{13}C NMR chemical shifts of NOCbl were completely assigned by ROESY, TOCSY, HSQC, and HMBC experiments. Molecular mechanics modelling of NOCbl was performed using the parameters derived specifically to model the cobalt corrins[38,39] as an extension of Allinger's MM2 force field.[40] Our results suggest that the electronic effects exerted by the NO ligand of NOCbl are closer to alkyl ligands rather than other inorganic ligands such as CN^-, NO_2^- and H_2O and that, consequently, a significant fraction of NOCbl in neutral solution exists in the DMB-deprotonated, base-off form.

Experimental

Synthesis of NOCbl

Both the synthesis and handling of NOCbl were carried out inside a glove box under an argon atmosphere. NOCbl was synthesized according to our published procedure,[23] with minor modifications. A freshly prepared anaerobic solution of HOCbl·HCl (35 mg HOCbl·HCl in 1 mL H_2O) was added to solid DEA-NONOate (8.73 mg, 2.5 equiv.). The product solution was shaken gently to ensure complete mixing and the reaction left to proceed at room temperature

for 12 h. The final pH of the mixture was 10.8. Formation of the desired product was checked by UV-vis and ^{1}H NMR spectroscopy.[23] The product was precipitated by drop-wise addition to cold acetone (20 mL, −20 °C), filtered and dried under vacuum (2×10^{-2} mbar) for 3 h. We observed that both the unreacted DEA-NONOate and the reaction product DEA-NO co-precipitated with NOCbl, with their corresponding ^{1}H NMR signals in the aliphatic region of the spectrum interfering with our measurements. Therefore, the acetone precipitation step (and dissolution back into H_2O) was repeated two more times, resulting in removal of most of the interfering compounds. NOCbl remained stable during the procedure, yielding a final purity of ~97% by ^{1}H NMR spectroscopy.

Preparation of the NOCbl NMR spectroscopy sample

NOCbl (35 mg) was dissolved in 0.80 mL of anaerobic phosphate buffer (0.15 M, pH 7.40) made up with 90% H_2O/10% D_2O, and containing 1 mg of TSP. The final pH of the sample was 7.70. The NMR tube was flame-sealed under vacuum and the purity of the sample checked by ^{1}H NMR spectroscopy. The sample was stable for at least 3 months at room temperature, in the dark, as assessed by ^{1}H NMR and UV-vis spectroscopy (the latter experiment requiring the NMR tube to be broken open and the sample diluted with anaerobic buffer prior to transferring to a Schlenk cuvette for a UV-vis spectroscopy measurement).

^{31}P NMR spectroscopy experiments

SO_3Cbl and NO_2Cbl were prepared using published procedures.[41] ^{31}P NMR spectroscopy measurements were made at 25 °C on a Bruker Avance 400 MHz spectrometer operating at 161.975 MHz. Samples (~6–7 mM) were dissolved in D_2O (1 ml), and chemical shifts externally referenced to an NMR tube containing 85% H_3PO_4 equipped with a concentric insert containing D_2O.

NOCbl 2-D NMR spectroscopy experiments

Two-dimensional homonuclear (TOCSY and ROESY) experiments with Watergate solvent suppression and heteronuclear (HSQC and HMBC) experiments for resonance assignment were carried out as previously described[30] on a Brucker DMX 600 NMR spectrometer. Assignments were made as described elsewhere.[42]

For molecular modelling distance restraints, ROESY spectra were obtained on a Brucker DRX 800 NMR spectrometer at mixing times of 40, 80, 120, and 160 ms.

Attempted determination of p$K_{\text{base-off}}$ for NO_2Cbl

^{1}H NMR spectra of samples of NO_2Cbl (5×10^{-3} M) in acidic solution (H_2SO_4 + D_2O) were recorded at 25 °C on a Bruker Avance 400 MHz spectrometer with TSP used as an internal reference.

Molecular modelling calculations

All modelling calculations (energy minimizations, MD runs and SA calculations) were performed with HYPERCHEM v. 7.03[43] using the potential energy functions of the MM+ force field (as MM2 is called in this suite of programs) and the parameters derived for the cobalt corrins.[38,39] Parameters for NO coordinated to Co(III) in NOCbl were not available. We therefore developed preliminary parameters based upon the crystal structures of NOCbl[23] and four Co(III)NO porphyrins.[44–47] NO is disordered over three positions in NOCbl; the mean N–O bond length is 1.18(3) Å. It is not significantly different in the CoNO porphyrins (1.14(6) Å). We used a value of k_s = 10.0 mdyn Å^{-1} for the bond force constant and l_o = 1.175 Å for the strain-free bond length for modelling the bond between N (atom type n1) and O (atoms type o1). In NOCbl, the Co–N bond length is 1.927 Å and shorter in CoNO

porphyrins (1.839(8) Å). We used k_s = 2.0 mdyn Å^{-1} and l_o = 1.865 Å in the force field. NO coordinates to Co(III) in a bent manner (Co–N–O = 120(2)° in NOCbl and is similar (122.9 (9)°) in CoNO porphyrins. The angle was modelled using an angle bending force constant k_b = 1.0 mdyn Å rad^{-2} and a strain free bond angle of θ_o = 116°.

A total of 64 NOE cross peaks (Table S1 †), not including those resulting from geminal hydrogens, could be resolved and assigned in the ROESY spectra in H_2O at the longest mixing time (160 ms) for NOCbl. These cross peaks were classified[48] as strong, medium, weak, or very weak, depending on whether they first appeared in the ROESY spectra at mixing times of 40, 80, 120, or 160 ms, respectively.

The crystal structure of NOCbl,[23] from which we excluded all solvent molecules, was used as starting point for the modelling. Energy minimization was performed using a Polak-Ribiere conjugate gradient algorithm with a convergence criterion of 0.01 kcal Å^{-1} mol^{-1} r.m.s. gradient.

We used a set of parabolic potential energy functions of the form $U_{NOE}(r_{ij}) = k_{NOE}(r_{ij} - r_{ij}^{o})^2$ to restrain the distance r_{ij} between protons i and j determined from the 2D ROESY spectra. Following the definition of Clore and co-workers,[49] and as we have explained elsewhere,[33] we used values of the restraining force constant, k_{NOE} = 1.2, 0.52, 0.3, and 0.075 kcal mol^{-1} Å^{-2} at 300 K for strong, medium, weak and very weak NOE's, respectively. Violations of these distance restraints were taken when $r_{ij} \geq$ 3.0, 3.8, 4.8 and 5.3 Å, respectively.

The assignments of all pro-chiral protons were made on a trial and error basis until the minimum number of violations of distance criteria were obtained during a series of 100 ps MD simulations at 300 K. Where a number of NOE's to the same achiral centre occur, care was taken to choose for each restraint the proton pair with the smallest inter-proton distance. The leapfrog algorithm[50,51] was used to solve the Newtonian equations of motion that describe the dynamics trajectory for MD simulation calculations. A small time step of 0.5 fs was used. Temperature scaling with coupling to an external heat sink[52] (using a temperature relaxation time of 0.1 ps), was used to control the temperature. Initial velocities for MD simulations were assigned to fully energy minimized structures using a random number generator. In a typical simulation, the molecule was heated from 0 K to the run temperature (300 or 800 K) during a 20 ps heating phase. The run phase at 800 K was varied between 1 and 750 ps for simulations designed to find stable conformations while a run phase of 500 ps was used to determine inter-proton distances at 300 K. The run phase was followed by an annealing phase of 20 ps to 0 K for simulations designed to find stable conformations, followed by full energy minimization. A consensus structure was obtained by averaging the coordinates of each atom of each of 25 annealed structures and then energy minimizing again.

Results and discussion

NMR spectroscopy measurements for NOCbl

2-D NMR experiments (TOCSY, ROESY, HSQC, and HMBC) allowed the complete assignment of the ^{1}H and ^{13}C NMR resonances for NOCbl in solution (pH 7.70, 25 °C). Table 1 summarizes the final ^{1}H and ^{13}C chemical shift assignments for NOCbl and Table S1† shows the 2-D NMR correlations which support these assignments. A labelling scheme for NOCbl is given in Fig. 1. Significant (≥1.0 ppm) ^{13}C chemical shift differences between NOCbl and two "normal" Co(III)Cbls with nitrogen-linked upper axial ligands, nitrocobalamin (NO_2Cbl) and amminocobalamin (NH_3Cbl), are summarized in Table 2. As 19 of 62 (31%) chemical shifts are significantly different, it is reasonable to conclude that NOCbl is not a typical Co(III)Cbl

†Electronic supplementary information (ESI) available: Table S1–S3 and Fig. S1. See DOI: 10.1039/b810895a

with a nitrogenous upper axial ligand. In particular, the chemical shift differences at the corrin ring carbons C15, C14, C9, C16, and C4 suggest significantly different corrin ring electronic effects in NOCbl.

As depicted in Scheme 1, in aqueous solution Cbls exist in three forms: base-on, base-off with the 5,6-dimethylbenzimidazole (DMB) deprotonated, and base-off with the DMB protonated. Under more acidic conditions, Cbl species that are mono and diprotonated at the phosphodiester also exist ($pK_a \sim -0.1$ and -1.6[53]). The ground state structural and thermodynamic *trans* influence of the β-axial ligand of Cbls is well established, with strong σ donor ligands resulting in long Co-NB3 bond distances, small K_{Co} values (Scheme 1) and higher $pK_{base\text{-}off}$ values.[54–56]

A $pK_{base\text{-}off}$ value of 5.1 was recently reported for NOCbl using UV-vis and ^{1}H NMR spectroscopy,[18] which is the highest reported value for any Cbl ($pK_{base\text{-}off}$ for other Cbls are in the −2.1 to 4.1 range[53]). We also obtained a similar value using ^{1}H NMR spectroscopy. Using $pK_{aBz} = 5.56$,[57] a value of $K_{Co} = 1.9$ is calculated; that is, under neutral conditions approximately one third of NOCbl exists in a DMB deprotonated, base-off form, Scheme 1.

It was of interest to us to determine $pK_{base\text{-}off}$ for NO_2Cbl for comparison purposes. To our knowledge, this value has not been reported. Upon conversion of Cbls to their base-off, protonated forms, large changes are observed in the aromatic region of the ^{1}H NMR spectrum.[18] However, measuring ^{1}H NMR spectra for acidic solutions of NO_2Cbl at varying pD values showed that hydrolysis of NO_2Cbl to H_2OCbl^+ occurs prior to formation of significant amounts of protonated, base-off NO_2Cbl. For example, at pD 0.8, only ~18% NO_2Cbl remains, with chemical shifts identical within experimental error to those for base-on NO_2Cbl at pD 6.7. Assuming that at this pD condition ≥90% NO_2Cbl is base-on, a value of $pK_{base\text{-}off} \leq -0.15$ is calculated. Hence unlike NOCbl, $pK_{base\text{-}off}$ NO_2Cbl is within the range expected for Cbls with inorganic ligands at the β-axial site ($pK_{base\text{-}off}$ (H_2OCbl^+) =−2.13, $pK_{base\text{-}off}$ (CNCbl) = 0.1[53,58]).

A linear relationship between the apparent Gibbs free energy for coordination of 5,6-dimethylbenzimidazole to cobalt, $-\Delta G_{Co}^{o}$, and the Co-NB3 bond distance, $d_{Co–NB3}$, has previously been established.[59,60] Using $K_{Co} = 1.9$, a value of 0.38 kcal mol^{-1} is calculated for NOCbl. Fig. 2 gives a plot of $-\Delta G_{Co}^{o}$ *versus* $d_{Co–NB3}$ for a series of Cbls, including NOCbl. $-\Delta G_{Co}^{o}$ is remarkably small for NOCbl, in accordance with the high $pK_{base\text{-}off}$ value. It is apparent from this plot that NOCbl deviates significantly from the line of best fit for other non-alkyl and alkylcobalamins, and is closer to that expected for an alkylcobalamin.

Given that the $pK_{base\text{-}off}$ value of 5.1 for NOCbl is unexpectedly high, it is informative to evaluate the importance of the DMB deprotonated, base-off conformation by other means. The chemical shift of the DMB carbons have been shown to be sensitive to the strength of coordination of the axial DMB to the cobalt atom in base-on Cbls.[61,62] Table 3 shows a comparison of the ^{13}C DMB chemical shifts of adenosylcobalamin (AdoCbl), methylcobalamin (CH_3Cbl), cyanocobalamin (CNCbl), and aquacobalamin (H_2OCbl^+) to those of NOCbl and those of two base-off (but DMB deprotonated) Cbls, dicyanocobalamin, $(CN)_2Cbl^-$ and α-AdoCbl (Ado (= 5′-deoxyadenosyl) ligand in the lower or α-axial position). Clearly, the DMB of NOCbl more closely resembles that of AdoCbl or CH_3Cbl, where the equilibrium constant for formation of the base-on species from the base-off, DMB deprotonated species, K_{Co}, is of the order of 10^1 to 10^2, than that of CNCbl or H_2OCbl^+ where K_{Co} is $>10^5$. Indeed, the ^{13}C NMR chemical shifts of the DMB of NOCbl are quite close to those of the base-off species $(CN)_2Cbl^-$ and α-AdoCbl, Table 3, which again suggests that the base-off, DMB deprotonated conformation of NOCbl (Scheme 1) is important in neutral, aqueous solution.

One of us has previously shown that for a series of 10 Cbls, the ^{13}C NMR chemical shift of the DMB carbons of the nucleotide loop also correlates directly with ΔG_{Co}^{o}.[61] Table 4 shows attempts to use the correlations of the DMB chemical shifts with the Gibbs free energy of formation of the base-on species, ΔG_{Co}^{o}, from this work to estimate the value of K_{Co} and $pK_{base\text{-}off}$ for NOCbl. The first three columns show the slope, intercept, and correlation coefficient of the correlation of each DMB carbon with ΔG_{Co}^{o} for the 10 Cbls studied. The B7 carbon was omitted, since the chemical shifts of the alkylcobalamins do not fall between those of XCbls (X = CN^-, H_2O) and the base-off Cbls. The B2 carbon was also omitted, since its chemical shift shows little dependence on ΔG_{Co}^{o}. The correlations for B4, B5, and B6 all give values of K_{Co} for NOCbl on the order of 10, *i.e.*, similar to an alkylcobalamin with a strongly electron donating alkyl ligand such as *n*PrCbl. The B8 and B9 correlations give K_{Co} values $\ll$ 1 for NOCbl, characteristic of a base-off Cbl. The value of 1.9 determined from $pK_{base\text{-}off}$ = 5.1 lies in between these two extremes. Importantly, although the lack of consistency of these estimates is somewhat disconcerting, it is consistent with NOCbl being an outlier, as observed in the $-\Delta G_{Co}$ *versus* $d_{Co–NB3}$ correlation (Fig. 2), and in the ^{31}P NMR chemical shift *versus* $d_{Co–NB3}$ correlation (Fig. 3, see below), albeit to a much lesser extent. Furthermore all of the correlations suggest that in solution NOCbl behaves more like an alkylcobalamin, with a covalent upper axial Co–X bond, than an inorganic Cbl with a dative Co–X bond, consistent with the deprotonated base-off conformation of NOCbl being an important species in neutral aqueous solution.

It has also previously been shown that the ^{31}P NMR chemical shift of the nucleotide phosphodiester moiety of Cbls correlates directly with the Co–NB3 bond distance.[53,59,63,64] The ^{31}P NMR chemical shift reflects changes in the phosphodiester bond angles, which become less strained as the Co–NB3 bond lengthens.[53,63] A plot of ^{31}P NMR chemical shift *versus* Co–NB3 bond distance, $d_{Co–NB3}$, is given in Fig. 3. In line with the $-\Delta G_{Co}^{o}$ *versus* $d_{Co–NB3}$ plot (Fig. 2), the ^{31}P NMR chemical shift of NOCbl is unexpectedly low and is closer to ^{31}P NMR shifts of alkylcobalamins rather than other Cbls with inorganic ligands. A single ^{31}P NMR resonance is observed for NOCbl under neutral and acidic conditions; hence on the NMR time scale, the base-on and base-off forms of NOCbl are in fast exchange, as observed for alkylcobalamins (CH_3Cbl, *n*PrCbl, CF_3CHCbl, CF_2HCbl, CF_3Cbl and $NCCH_2$Cbl[53]). The same is not true for CNCbl and H_2OCbl$^+$, for which two distinct peaks corresponding to the base-on and base-off, DMB protonated forms are observed in acidic solution at pH(pD) values close to $pK_{base\text{-}off}$[53,58]

Large spectral shifts of the αβ band region (400–600 nm) of the UV-visible spectrum to higher energy accompanied by a colour change from red to yellow occur upon conversion of base-on XCbls to their deprotonated (or protonated) base-off forms.[65] In Fig. 4, the UV-vis spectrum of NOCbl is compared with MeCbl, protonated base-off MeCbl, CNCbl and NO_2Cbl. The αβ band region of NOCbl is noticeably shifted towards shorter wavelengths compared with the other XCbls with inorganic ligands (X = CN^-or NO_2^-), providing further compelling evidence that the base-off, DMB-deprotonated form is especially important for NOCbl under neutral pH conditions. The spectral differences observed in Fig. 4 are also reflected in the colours of the solutions. Whilst CNCbl ($K_{Co} > 10^5$, Scheme 1) and NO_2Cbl are red, MeCbl (K_{Co} = 467) is red-orange, NOCbl (K_{Co} = 1.9) is bright orange and base-off, protonated MeCbl is yellow.

Importantly, there was no evidence for a deprotonated, base-off NOCbl species in the X-ray diffraction electron density map for NOCbl;[23] hence it appears that significant amounts of this form occurs in solution only. However, the finding that the NO ligand behaves electronically more like an alkyl ligand rather than a typical inorganic ligand is supported by the X-ray structural data. For NOCbl, the Co–NB3 bond length is 2.13 Å,[23] which is similar in length to that reported for MeCbl (2.16 Å[66]). The Co–NB3 bond lengths for Cbls with typical inorganic

ligands such as CN^-, NO_2^-, H_2O and N-acetyl-L-cysteine are 2.01–2.04, 1.99–2.01, 1.93, and 2.06 Å, respectively.[41,67–70] In pentammine complexes of Co, $[CoX(NH_3)_5]^{n+}$, NO was found to exert an even stronger *trans* influence than Me.[71] Interestingly, the Co–NB3 bond distance for AdoCbl (2.24 Å[72]) is considerably longer than that for MeCbl (2.16 Å[66]). Finally, like NOCbl, sulfitocobalamin (SO_3Cbl) also has a longer Co–NB3 bond distance (2.13–2.15 Å[73,74]) compared with other Cbls with β-axial inorganic ligands. The longer Co–NB3 for SO_3Cbl and NOCbl can be attributed to the strong σ donor properties of these ligands, in addition to NO being a moderately good π acceptor ligand.[75]

Molecular dynamics and simulated annealing

Table S2† lists all the NOE's, their assigned strength, and the average, standard deviation, maximum, minimum and median H–H distances during a 500 ps molecular dynamics simulation at 300 K of the base-on form of NOCbl. Given the clear importance of a base-off form of NOCbl in solution (*vide supra*) we then broke the Co–NB3 bond and repeated the simulation for the base-off form; the data are also listed in Table S2.

The modelling accords well with the solution structure of NOCbl. Of the 64 NOE's only 3 (4.7%) violate the distance criteria outlined above in both the base-on and the base-off forms of NOCbl. The distance between C26′ and C3 (2.55 and 2.56 Å on average for the base-on and base-off forms, respectively) accords with a strong NOE, but that between C3 and C26″ is too long (3.53 Å for both forms of NOCbl); this is in line with the relative inflexibility we see in the *a* side chain (*vide infra*). The C53 and C18 protons are well separated (the average modelled distance is 5.08 Å for base-on NOCbl and 5.24 Å for base-off NOCbl); that this gives rise to a clear, albeit weak NOE, is puzzling. The average modelled distance between the B7 proton and the proton on R4 is long even for a very weak NOE (5.67 and 5.69 Å for base-on and base-off NOCbl, respectively) but we note the wide range of inter-proton distances (6.41 to 2.32 Å, and 6.41 to 4.42 Å, respectively) and the relatively large standard deviation of the distance (0.21 and 0.25 Å, respectively) and conclude that the violation is marginal.

Two NOE's violate the distance criteria in the base-on form of NOCbl. The distance violation between C56′ and C18 is marginal in the base-on form (the average distance is 3.36 Å) but is very well accounted for in the base-off form (average 2.56 Å). The distance between the f_H proton and that on R3 (5.09 Å in the base-on form) is too long for even a weak NOE, but is also well accounted for in the modelling of the base-off form (3.04 Å). There is a single NOE that is compatible only with the base-on form. The weak NOE between C56″ and the R4 proton cannot be due to the base-off form (average 5.92 Å) but is within the expected distance in the base-on form (average 4.53 Å).

Simulated annealing calculations were performed on both the base-on form of NOCbl (omitting the C56′–C18 and the f_H–R3 NOE's) and the base-off form (omitting the C56″–R4 NOE). Fig. 5A shows 25 annealed structures for base-on NOCbl overlaid at the Co ion and four corrin N donor atoms. Two views of the consensus structure of base-on NOCbl are shown in Fig. 6A and 6B (in black) overlaid with the crystal structure of NOCbl (white). Base-off NOCbl annealed into two principal conformations. In the first (Fig. 5C; the consensus structure is shown in Fig. 6D) the base is perpendicular to the corrin and the B3 nitrogen is about 3.1 Å away from and pointing directly at the metal ion. In the second structure (Fig. 5B, consensus structure in Fig. 6C), the base is virtually parallel to and tucked beneath the D ring of the corrin. Two other annealed structures in which the base is more remote from the metal were also identified and are shown in Fig. 5D.

Structural metrics

In Table S3† we compare some structural metrics of the base-on consensus structure and the crystal structure. The O atom of the NO ligand in the modelled structures, as in the crystal structure, occupies three different positions. When we developed the force field parameters for modelling the corrins[38] we surveyed the structures of the then available Co(III) corrins and based our force field parameters on the averages of the structural metrics. We found that the average Co–N bond length to N21 and N24 is 1.885(38) Å, whilst that to N22 and N23 is longer, 1.924(44) Å. This is well-reproduced in the modelling of NOCbl (Table S3). The Co–N bond length to coordinated NO and the N–O bond lengths are well-reproduced (1.175 *versus* an average of 1.176 Å in the X-ray structure). The Co–NB3 bond length to coordinated DMB in the consensus structure (2.063 Å) is significantly shorter than that observed in the X-ray structure of NOCbl (2.123 Å). It is well established that the Co–NB3 bond length is influenced by the electronic donor power of the *trans* β ligand.[54,55] Since MM methods are insensitive to such electronic effects, when modelling alkylcobalamins[27] we use a different parameter for the Co–NB3 bond (k_s = 2.8 mdyn Å^{-1}, l_o = 2.138 Å) than when modelling cobalt corrins where the β ligand is an "inorganic" moiety such as CN^-, H_2O or $S_2O_3^{2-}$ (k_s =2.8 mdyn Å^{-1}, l_o = 2.010 Å) The Co–NB3 bond length of 2.063 Å (or 0.06 Å too short) was produced using the "inorganic" parameter; it increased to 2.173 Å (*i.e.*, 0.05 Å too long) when we used the parameter appropriate for modelling alkylcobalamins. Thus, NO behaves in NOCbl somewhat like an alkyl ligand of moderate *trans* influence. For convenience, all modelling was performed with the "inorganic" parameters and the axial bond lengths to coordinated DMB are too short by about 0.06 Å.

The C–N bond lengths observed in the X-ray structure of NOCbl are within the range for cobalt corrins (N21–C1, N24–C19, 1.49(4) Å; N21–C4, N24–C16, 1.31(4) Å; N22, N23–C, 1.37(5) Å) and are well reproduced in the modelling. The same is true for the C–C bonds with double bond character (crystallographic mean 1.40(7) Å) and the C–C single bonds (crystallographic mean 1.55(6) Å).

Bond angles are generally well-reproduced (Table S3†); the average difference between the base-on consensus structure and the solid state structure is 1.5° and 85% of the bond angles reported in Table 2 are reproduced to better than 2.5°.

The corrin fold angle is defined as the angle between the mean planes through N21, C4, C5, C6, N22, C9 and C10, and through N24, C16, C15, C14, N23, C11 and C10.[76] In the X-ray structure of NOCbl the corrin has a fold angle of 15.9°. The consensus structure is slightly more folded (16.8°) and changing the parameters for modelling the Co–NB3 bond thus elongating that bond (vide supra) changes the fold to 15.3°, lower than the X-ray structure value. The fold angles of the 25 annealed structures from which the consensus structure was derived vary between 9.8° and 18.9° (mean 14.4(3.1)°).

The annealed structures

The annealed structures illustrated in Fig. 5 provide insight into the considerable flexibility of NOCbl. In both the base-on and base-off forms, the O atom of the NO ligand occupies one of three positions, very similar to the positions observed in the crystal structure. In the base-on form the *a*, *d* and *g* side chains are all in approximately the same orientation, whilst the *b*, *c* and *e* side chains occupy a number of orientations. In the base-off form the *a* and *d* side chains are more flexible. In the base-on form the greatest variability is seen in the *f* side chain and the nucleotide loop; this leads to a variety of dispositions of the ribose and DMB relative to the corrin. Fig. 7 shows the extremes; at one extreme DMB is parallel to the C5 ···C15 line and the ribose is beneath the C15–C16 bond and at the other extreme DMB has rotated by 17° in a counter clockwise fashion towards C4 when viewed from above the corrin and the ribose is

nearly beneath the C ring. We have previously noted this considerable flexibility in the *f* side chain in the modelling of other cobalamins.[37]

There is little variation in the A ring of the corrin in the base-on form. C1, N21 and C4 are planar with C2 and C3 below the plane. Similarly, in the B ring C6, N22 and C9 are planar, C7 is above the plane and C8 below. On the other hand, both the C and D rings show considerable flexibility. The C ring adopts a range of conformations. At one extreme the ring is virtually planar, and both the C46 and C47 methyl groups are in a pseudo equatorial position. At the other, C11, N23 and C14 are planar, C12 is above the plane so that the C46 methyl group is in an axial position whilst the C47 methyl is equatorial, and C13 is below the plane. The D ring adopts a range of conformations between two extremes. In the first, C16, N24, C17 and C19 are virtually coplanar and C18 is displaced towards the α face of the corrin, whilst in the second C17, C18, C19 and N24 are coplanar and C16 is displaced towards the β face.

As might be expected, untethering of the nucleotide loop imparts greater flexibility to the corrin, and especially the *f* side chain; however, in all annealed structures of the base-off form of NOCbl that we obtained DMB remains close to the α face of the corrin. Annealing produced structures that fit broadly into one of three classes. In the first (13 of the 25 structures, 52%, Fig. 5B) DMB is *anti* to the ribose, and nearly parallel to the corrin beneath the A ring (Fig. 6C shows the consensus structure). The distance between NB3 and Co ranges between 7.4 and 8.3 Å (average 7.9(2) Å; 7.78 Å in the consensus structure). In the second (10 structures, 30%, Fig. 5C), DMB is perpendicular to the corrin with the distance between Co and NB3 between 2.9 and 3.8 Å (3.11 Å in the consensus structure, Fig. 6D). In two structures (8%, Fig. 5D) DMB annealed *syn* to ribose and is nearly parallel to the corrin. As only two structures were found we could not determine a consensus structure for what is likely to be a minor conformation of base-off NOCbl.

In a 250 ps dynamics simulation at 300 K, in which the distance between Co and NB3 and between C20 and NB3 was monitored every 10 fs, the largest distance between Co and NB3 was 8.35 Å and that between C20 and NB3 was 5.94 Å (see Figure S1 of the ESI[†]). If all the NOE's are removed, the nucleotide loop swung out by rotating about the Pr1–Pr2 bond (see Fig. 1) and the structure energy-minimised, the distance between C20 and NB3 is over 17 Å whilst the Co ···NB3 distance is over 18 Å. Hence the 300 K dynamics simulation shows that DMB remains tucked in near the α face throughout the dynamics trajectory. Removing the weak NOE between C56″H and R4H, which is unique to the base-off species, and repeating the dynamics trajectory does not significantly alter the results. It is clear that, probably because of the sentinel-like effect of the three propionamide side chains and the C20 methyl that point downward towards the α face, the DMB ligand does not readily move from the vicinity of the corrin's α face. These results are in broad agreement with those we obtained previously when we modelled a base-off cobalamin, methyl-3,5,6-trimethylbenzimidazolylcobamide ($CH_3Me_3BzmCba^+$), in which the B3 nitrogen of DMB is blocked by a methyl group.[33] In that case we found that in the absence of tethering by the metal ion, the nucleotide loop has considerable motional freedom but that in an extended dynamics simulation at 300 K the base also remains near the α face of the corrin.

Conclusion

^1H and ^{13}C NMR chemical shifts of NOCbl have been assigned using 2-D NMR techniques. Interproton distances obtained by NOE experiments have been used in conjunction with molecular mechanics to obtain the structure of NOCbl in solution, with over 95% agreement between the resulting structures and the NOE data. ^{13}C and ^{31}P NMR chemical shifts, $pK_{base\text{-}off}/-\Delta G_{Co}{}^{o}$ and UV-vis spectra of NOCbl compared with other Cbls suggest that the NO ligand has electronic properties significantly differing from inorganic ligands such as

CN^- or H_2O, closer to the covalently bound alkyl ligands of alkylcobalamins. Furthermore, $pK_{base\text{-}off}$, ^{13}C NMR shifts and the visible spectrum of NOCbl are consistent with the base-off DMB deprotonated form being much more important for NOCbl in solution compared with all other known Cbl species, including alkylcobalamins. Molecular modelling was performed separately on a base-on and on a base-off form of NOCbl. The solution structure of the base-on form is similar to that observed by X-ray diffraction, with minor differences in the conformationally flexible side chains and in the position of the nucleotide loop. Modelling of the base-off form shows that DMB can adopt a range of positions relative to the corrin, but remains in close proximity of the macrocycle's α face. It was not possible to obtain a reliable estimate of the Co–NB3 bond distance from the molecular mechanics calculations, since these calculations do not take into account electronic effects experienced by the Co–NB3 from the β-axial NO (the *trans* influence); however MM calculations using parameters typical for either β-axial inorganic or alkyl ligands provide further support that NO has electronic properties between those of inorganic and alkyl ligands.

Supplementary Material

Refer to Web version on PubMed Central for supplementary material.

Acknowledgments

We wish to acknowledge funding of this research from Kent State University (NEB), the South African Department of Science and Technology and the National Research Foundation, Pretoria, (HMM), the University of the Witwatersrand (HMM), and the Egyptian Ministry of Higher Education (HAH).

References

1. Banerjee, R., editor. Chemistry and Biochemistry of B_{12}. Wiley; New York: 1999.
2. Carmel, R. Homocysteine in Health and Disease. Jacobsen, DW.; Carmel, R., editors. Cambridge University Press; Cambridge: 2001. p. 289-305.
3. Brouwer M, Chamulitrat W, Ferruzzi G, Sauls DL, Weinberg JB. Blood 1996;88:1857–1864. [PubMed: 8781445]
4. Wheatley C. Med Hypotheses 2006;67:124–142. [PubMed: 16545917]
5. Wheatley C. J Nutr Environ Med 2007;16:181–211. [PubMed: 18836533]
6. Valko M, Rhodes CJ, Moncol J, Izakovic M, Mazur M. Chem Biol Interact 2006;160:1–40. [PubMed: 16430879]
7. McInnes, IB.; Liew, FY. Nitric Oxide in Bone and Joint Disease. Hukkanen, MVJ.; Polak, JM.; Hughes, SPF., editors. Cambridge University Press; Cambridge: 1998. p. 8-20.
8. Rand MJ, Li CG. Eur J Pharmacol 1993;241:249–254. [PubMed: 8243559]
9. Greenberg SS, Xie J, Zatarain JM, Kapusta DR, Miller MJ. J Pharmacol Exp Ther 1995;273:257–265. [PubMed: 7714773]
10. Schubert R, Krien U, Wulfsen I, Schiemann D, Lehmann G, Ulfig N, Veh RW, Schwarz JR, Gago H. Hypertension 2004;43:891–896. [PubMed: 14993195]
11. Jiang F, Li CG, Rand MJ. Eur J Pharmacol 1997;340:181–186. [PubMed: 9537813]
12. Weil M, Abeles R, Nachmany A, Gold V, Michael E. Cell Death Differ 2004;11:361–363. [PubMed: 14685162]
13. Nicolaou A, Kenyon SH, Gibbons JM, Ast T, Gibbons WA. Eur J Clin Invest 1996;26:167–170. [PubMed: 8904527]
14. Nicolaou A, Ast T, Garcia CV, Anderson MM, Gibbons JM, Gibbons WA. Biochem Soc Trans 1994;22:296S. [PubMed: 7821555]
15. Danishpajooh IO, Gudi T, Chen Y, Kharitonov VG, Sharma VS, Boss GR. J Biol Chem 2001;276:27296–27303. [PubMed: 11371572]

16. Kambo A, Sharma VS, Casteel DE, Woods VL Jr, Pilz RB, Boss GR. J Biol Chem 2005;280:10073–10082. [PubMed: 15647267]
17. Nicolaou A, Waterfield CJ, Kenyon SH, Gibbons WA. Eur J Biochem 1997;244:876–882. [PubMed: 9108260]
18. Wolak M, Zahl A, Schneppensieper T, Stochel G, van Eldik R. J Am Chem Soc 2001;123:9780–9791. [PubMed: 11583539]
19. Zheng D, Birke RL. J Am Chem Soc 2001;123:4637–4638. [PubMed: 11457265]
20. Zheng D, Birke RL. J Am Chem Soc 2002;124:9066–9067. [PubMed: 12149007]
21. Zheng D, Yan L, Birke RL. Inorg Chem 2002;41:2548–2555. [PubMed: 11978125]
22. Wolak M, Stochel G, van Eldik R. Inorg Chem 2006;45:1367–1379. [PubMed: 16441149]
23. Hannibal L, Smith CA, Jacobsen DW, Brasch NE. Angew Chem Int Ed Engl 2007;46:5140–5143. [PubMed: 17542034]
24. Wolak M, Stochel G, Hamza M, van Eldik R. Inorg Chem 2000;39:2018–2019. [PubMed: 12526506]
25. Roncaroli F, Shubina TE, Clark T, van Eldik R. Inorg Chem 2006;45:7869–7876. [PubMed: 16961380]
26. Holleman-Wiberg. Inorganic Chemistry. Vol. 34. Wiberg, N., editor. Academic Press, Walter de Gruyter; Berlin: 2001. p. 1582-1587.
27. Marques HM, Brown KL. Inorg Chem 1995;34:3733–3740.
28. Brown KL, Marques HM. Polyhedron 1996;15:2187–2197.
29. Brown KL, Cheng S, Marques HM. Inorg Chem 1995;34:3038–3049.
30. Brown KL, Cheng S, Marques HM. Polyhedron 1998;17:2213–2224.
31. Brown KL, Cheng S, Zou X, Chen G, Valente EJ, Zubkowski JD, Marques HM. Biochemistry 1998;37:9704–9715. [PubMed: 9657683]
32. Marques HM, Hicks RP, Brown KL. J Chem Soc Chem Commun 1996:1427–1428.
33. Brown KL, Zou X, Marques HM. J Mol Struct (Theochem) 1998;453:209–224.
34. Marques HM, Brown KL. J Mol Struct 2000;520:75–95.
35. Brown KL, Zou X, Chen GD, Xia ZP, Marques HM. J Inorg Biochem 2004;98:287–300. [PubMed: 14729309]
36. Brown KL, Zou X, Banka RR, Perry CB, Marques HM. Inorg Chem 2004;43:8130–8142. [PubMed: 15578853]
37. Perry CB, Brown KL, Zou X, Marques HA. J Mol Struct 2005;737:245–258.
38. Marques HM, Brown KL. J Mol Struct (Theochem) 1995;340:97–124.
39. Marques HM, Warden C, Monye M, Shongwe MS, Brown KL. Inorg Chem 1998;37:2578–2581.
40. Allinger NL. J Am Chem Soc 1977;99:8127–8134.
41. Suarez-Moreira E, Hannibal L, Smith CA, Chavez RA, Jacobsen DW, Brasch NE. Dalton Trans 2006:5269–5277. [PubMed: 17088966]
42. Brown KL. Chapter 7:197.Ref. 1
43. HYPERCHEM. Hypercube, Inc.; Gainesville, FL: 2002.
44. Kadish KM, Ou Z, Tan X, Boschi T, Monti D, Fares V, Tagliatesta P. J Chem Soc, Dalton Trans 1999:1595–1602.
45. Ellison MK, Scheidt WR. Inorg Chem 1998;37:382–383. [PubMed: 11670283]
46. Godbout N, Sanders LK, Salzmann R, Havlin RH, Wojdelski M, Oldfield E. J Am Chem Soc 1999;121:3829–3844.
47. Jene PG, Ibers JA. Inorg Chem 2000;39:5796–5802. [PubMed: 11151382]
48. Clore GM, Gronenborn AM. Science 1991;252:1390–1399. [PubMed: 2047852]
49. Clore GM, Brünger AT, Karplus M, Gronenborn AM. J Mol Biol 1986;191:553–561. [PubMed: 3029387]
50. Allen, MP.; Tildesley, DJ. Computer Simulation of Liquids. Claredon; Oxford: 1987.
51. Saiz E, Tarazona MP. J Chem Educ 1997;74:1350–1354.
52. Berendsen HJC, Postma JPM, van Gunsteren WF, DiNola A, Haak JR. J Chem Phys 1984;81:3684–3690.

53. Brown KL, Hakimi JM, Jacobsen DW. J Am Chem Soc 1984;106:7894–7899.
54. Kratky C, Kraeutler B. Chapter 2:9.Ref. 1
55. Pratt, JM. Inorganic Chemistry of Vitamin B_{12}. Academic Press; London, New York: 1972.
56. Hayward GC, Hill HAO, Pratt JM, Vanston NJ, Williams RJP. J Chem Soc 1965:6485–6493.
57. Brown KL, Hakimi JM, Nuss DM, Montejano YD, Jacobsen DW. Inorg Chem 1984;23:1463–1471.
58. Brown KL, Hakimi JM. Inorg Chem 1984;23:1756–1764.
59. Brown KL, Evans DR, Zubkowski JD, Valente EJ. Inorg Chem 1996;35:415–423. [PubMed: 11666223]
60. McCauley KM, Pratt DA, Wilson SR, Shey J, Burkey TJ, van der Donk WA. J Am Chem Soc 2005;127:1126–1136. [PubMed: 15669852]
61. Brown KL, Hakimi JM. J Am Chem Soc 1986;108:496–503.
62. Note that in this paper the assignments of the B5 and B6 carbons are interchanged as this work was completed prior to the availability of NMR methods for the unambiguous assignment of ^{13}C resonances in Cbls.
63. Brown KL. Inorg Chem 1986;25:3111–3113.
64. Rossi M, Glusker JP, Randaccio L, Summers MF, Toscano PJ, Marzilli LG. J Am Chem Soc 1985;107:1729–1738.
65. Chemaly SM, Pratt JM. J Chem Soc, Dalton Trans 1980:2267–2273.
66. Randaccio L, Furlan M, Geremia S, Slouf M, Srnova I, Toffoli D. Inorg Chem 2000;39:3403–3413. [PubMed: 11196881]
67. Kraeutler B, Konrat R, Stupperich E, Faerber G, Gruber K, Kratky C. Inorg Chem 1994;33:4128–4139.
68. Garau G, Geremia S, Marzilli LG, Nardin G, Randaccio L, Tauzher G. Acta Crystallogr Sect B: Struct Sci 2003;B59:51–59.
69. Perry CB, Fernandes MA, Brown KL, Zou X, Valente EJ, Marques HM. Eur J Inorg Chem 2003:2095–2107.
70. Kratky C, Faerber G, Gruber K, Wilson K, Dauter Z, Nolting HF, Konrat R, Kraeutler B. J Am Chem Soc 1995;117:4654–4670.
71. Randaccio L, Geremia S, Nardin G, Wuerges J. Coord Chem Rev 2006;250:1332–1350.
72. Ouyang L, Rulis P, Ching WY, Nardin G, Randaccio L. Inorg Chem 2004;43:1235–1241. [PubMed: 14966957]
73. Randaccio L, Geremia S, Nardin G, Slouf M, Srnova I. Inorg Chem 1999;38:4087–4092.
74. Randaccio L, Geremia S, Stener M, Toffoli D, Zangrando E. Eur J Inorg Chem 2002:93–103.
75. Bultitude J, Larkworthy LF, Mason J, Povey DC, Sandell B. Inorg Chem 1984;23:3629–3633.
76. Glusker, JP. B_{12}. Dolphin, D., editor. Vol. 1. Wiley-Interscience; New York: 1982. p. 23-107.
77. Brown KL, Zou X. J Am Chem Soc 1992;114:9643–9651.
78. Brown KL, Brooks HB, Gupta BD, Victor M, Marques HM, Scooby DC, Goux WJ, Timkovich R. Inorg Chem 1991;30:3430–3438.
79. Zou X, Brown KL. Inorg Chim Acta 1998;267:305–308.
80. Bouquiere JP, Finney JL, Savage HFJ. Acta Crystallogr Sect B: Struct Sci Section B: Structural Science 1994;B50:566–578.
81. Pagano TG, Marzilli LG, Flocco MM, Tsai C, Carrell HL, Glusker JP. J Am Chem Soc 1991;113:531–542.
82. Wagner T, Afshar CE, Carrell HL, Glusker JP, Englert U, Hogenkamp HPC. Inorg Chem 1999;38:1785–1794. [PubMed: 11670948]

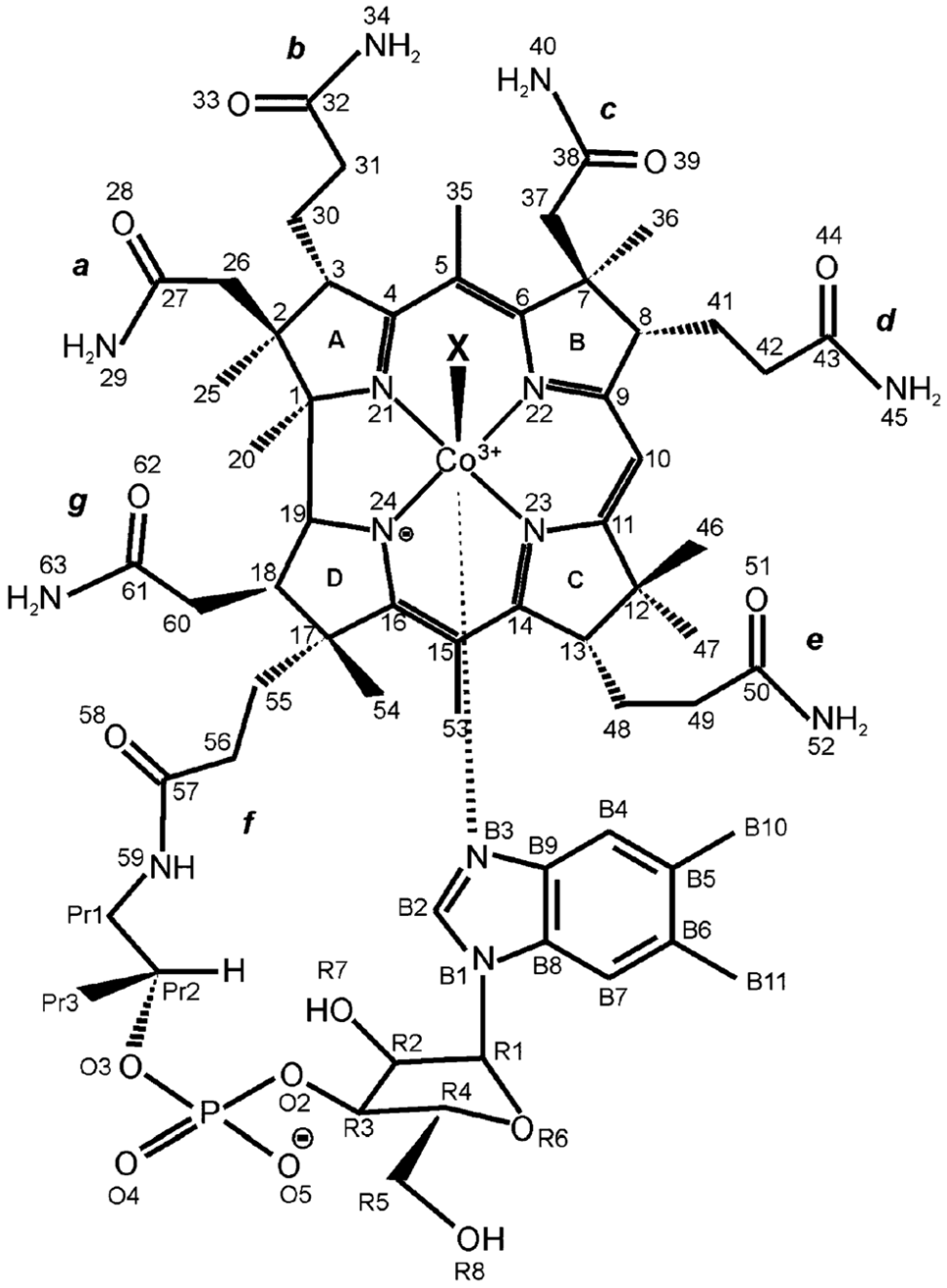

Fig. 1.
Labeling scheme for cobalamins. X = Me, Ado, H_2O, CN, NO, NH_3, NO_2, SO_3 *etc.*

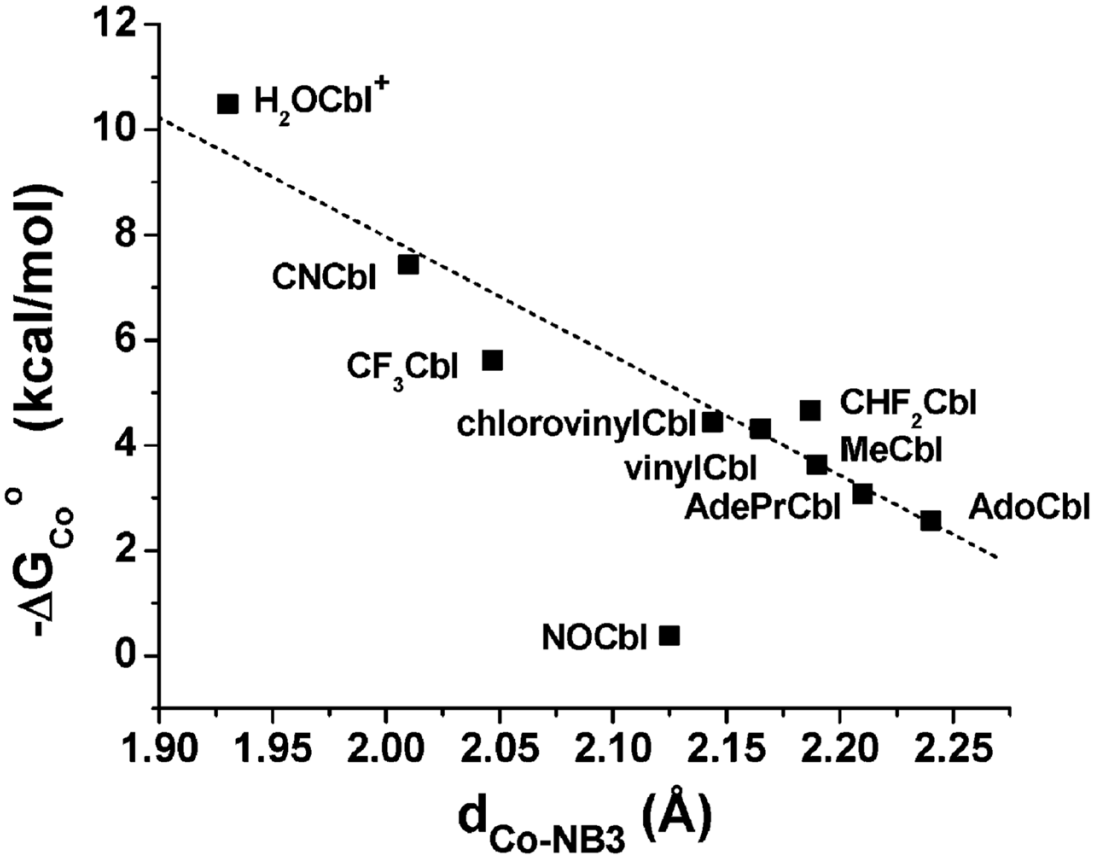

Fig. 2.

Plot of $-\Delta G_{Co}{}^{o}$ *versus* the Co–NB3 bond distance for Cbls. The data has been fitted to a straight line (r^2 = 0.93; data for NOCbl excluded) with slope = −22.6 ± 2.4 and intercept 53.2 ± 5.1. Co-NB3 bond lengths and $-\Delta G_{Co}{}^{o}$ values are taken from the literature.[23,53,59,60,66,67,70,79,80–82]

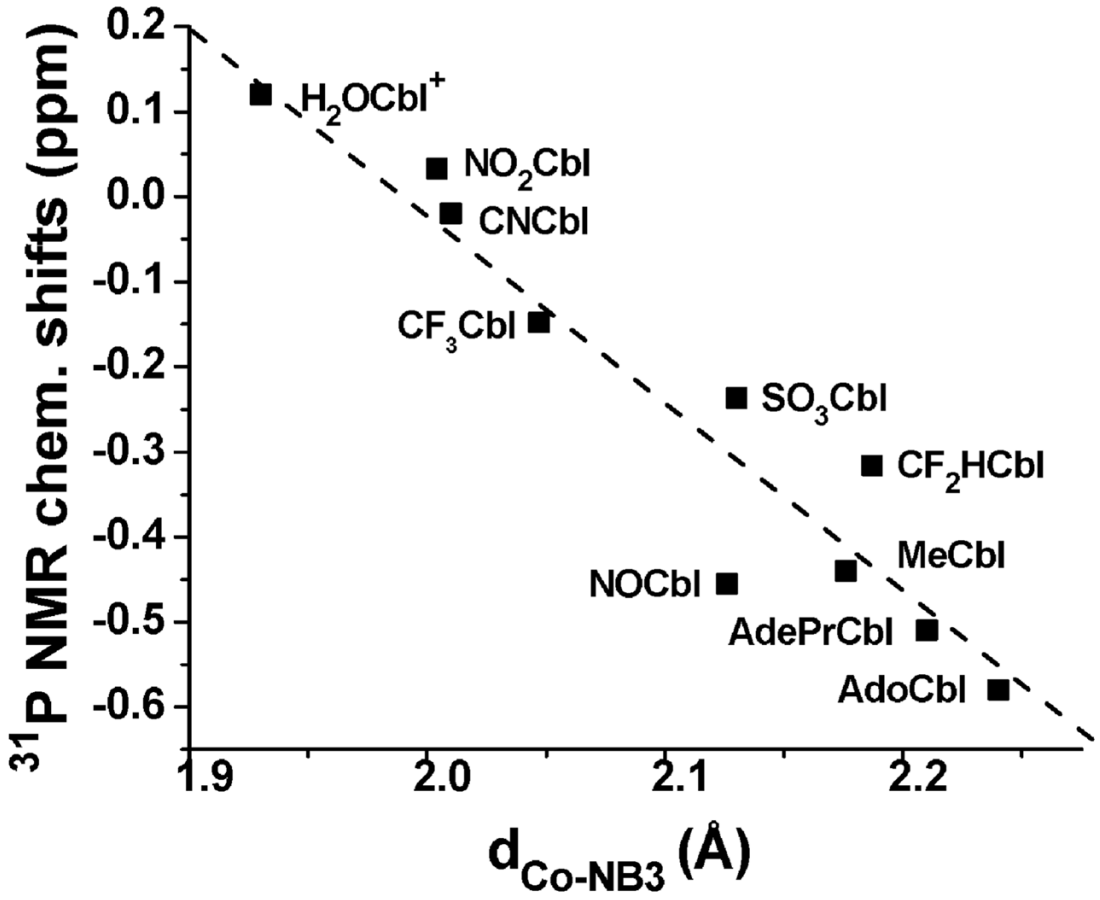

Fig. 3.

Plot of ^{31}P NMR chemical shift *versus* the Co–NB3 bond distance for Cbls (in D_2O or H_2O, referenced to 85% H_3PO_4, 25 °C). The data has been fitted to a straight line (r^2 = 0.91) with slope = −2.26 ± 0.26 and intercept 4.51 ± 0.54. ^{31}P NMR chemical shifts for SO_3Cbl (−0.24 ppm) NO_2Cbl (0.03 ppm) and NOCbl (−0.45 ppm, in excellent agreement with a literature value[18]) were determined in this study. All other ^{31}P NMR chemical shift data taken from the literature.[53,59] Co–NB3 bond lengths taken from reported structures.[23,64,66–68,70,73,79–82]

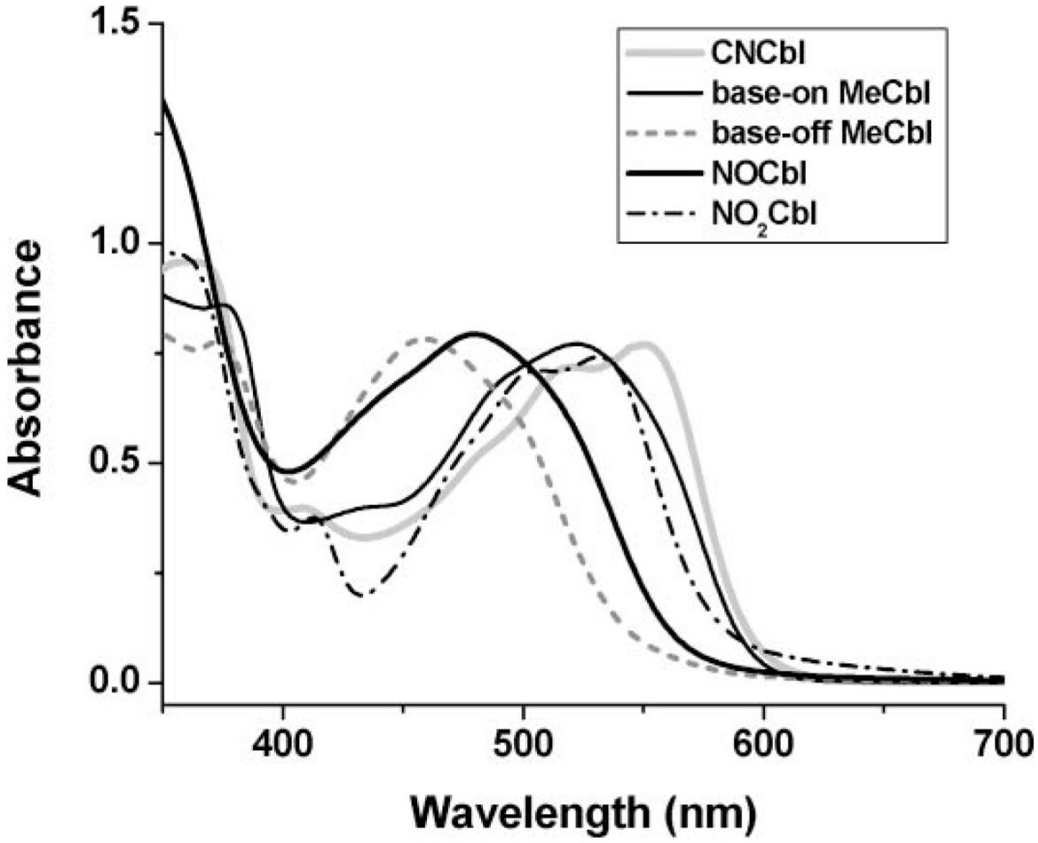

Fig. 4.
Visible region spectra of selected Cbls (6.0×10^{-5} M) in H_2O or at pH 1.37 (base-off MeCbl only), 25°C.

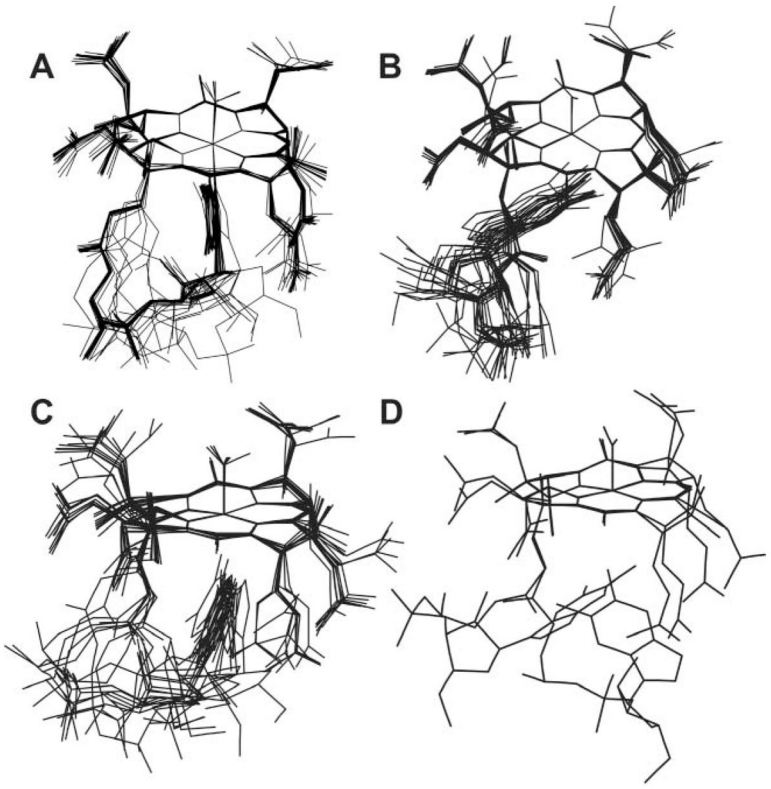

Fig. 5.

Superposition at the Co centre and the four corrin N atoms of (A) 25 annealed structures of base-on NOCbl; (B) 13 annealed structures of base-off NOCbl with DMB parallel to corrin and *anti* to ribose; (C) 10 annealed structure of base-off NOCbl with DMB perpendicular to corrin; and (D) 2 annealed structures of base-off NOCbl with DMB parallel to corrin and *syn* to ribose.

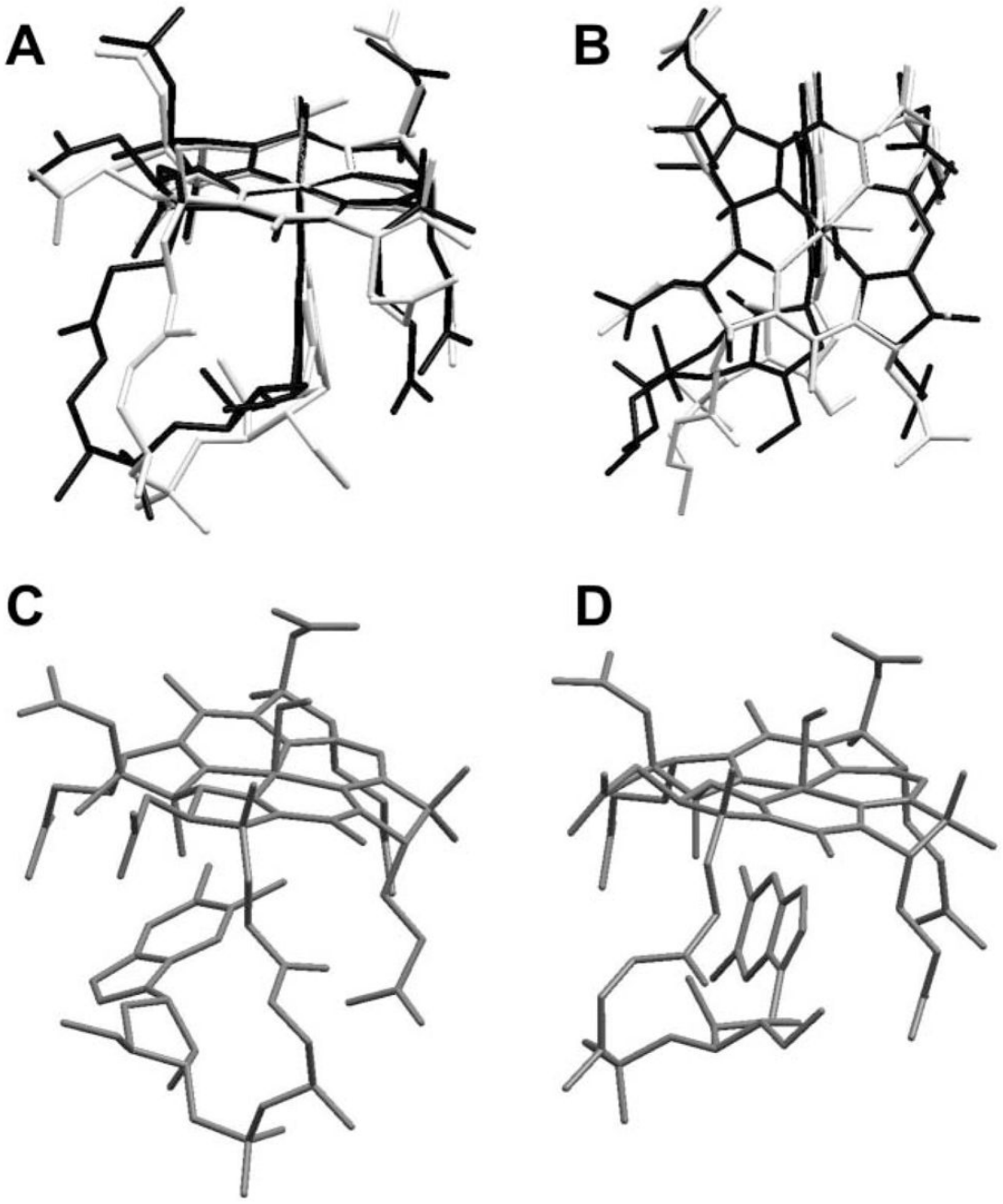

Fig. 6.

(A) and (B) show two views of the consensus structure obtained from MD/SA calculations of base-on NOCbl (dark lines) overlaid with the crystal structure of NOCbl (light lines). (C) and (D) show the consensus structures of the two main classes of structures into which base-off NOCbl annealed.

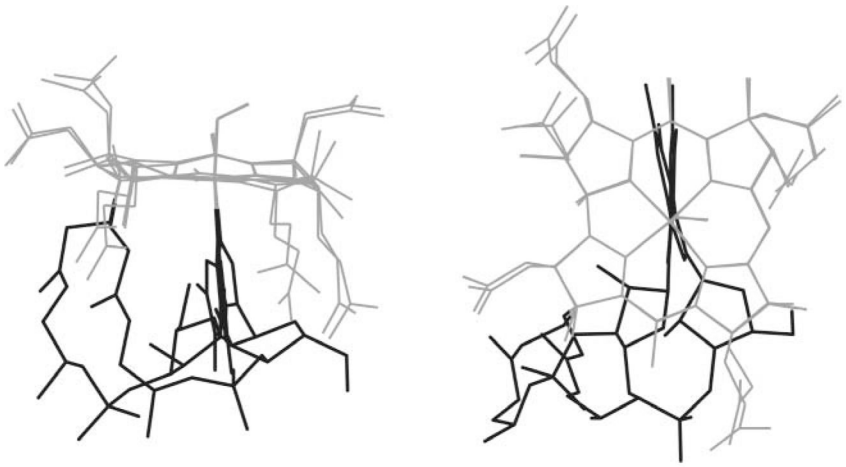

Fig. 7.

Superposition of base-on NOCbl showing the extremes of the orientation of the *f* side chain and the nucleotide loop in the annealed structure. This results in a range of orientations of the ribose and the DMB relative to the corrin.

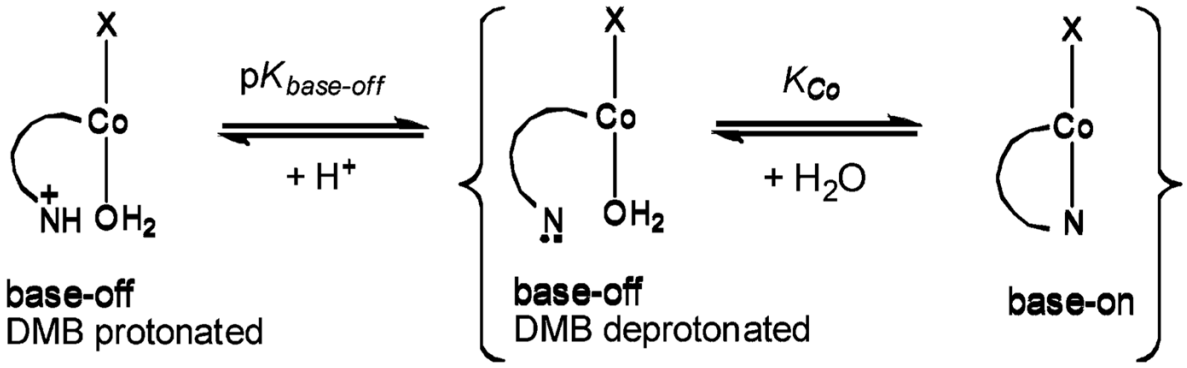

Scheme 1.
Cobalamin forms present in aqueous solution.

Table 1

^{1}H and ^{13}C NMR assignments for NOCbl[a]

Group	δ ^{13}C (ppm)	δ ^{1}H (ppm)	Group	δ ^{13}C (ppm)	δ ^{1}H (ppm)
C53	17.87	2.42	R1	88.51	6.26[e]
C35	18.03	2.51	C10	97.40	6.34
C25	19.39	1.39	C15	107.60	
C54	20.34	1.30	C5	109.91	
Pr3	21.42[b]	1.24[c]	B7	113.43	7.19
C36	22.09	1.82	B4	121.29	6.77
C47	22.09	1.50	B5	133.99	
B10	22.24	2.11	B8	134.21	
B11	22.24	2.11	B6	135.75	
C20	24.48	0.54	B9	142.20	
C30	28.50	1.89, 2.01	B2	144.53	7.44
C41	28.91	1.40, 2.04	C14	166.30	
C48	29.25	1.88, 2.03	C6	166.40	
C46	34.33	0.98	C9	174.53	
C55	34.78	1.81, 2.37	C38	177.36	
C42	34.78	1.72, 2.06	C57	177.91	
C31	34.95	2.47, 2.73	C16	178.23	
C56	34.95	1.87, 2.47	C27	178.71	
C49	36.04	2.20, 2.35	C11	178.71	
C60	37.86	2.52, 2.56	C4	178.71	
C18	41.88	2.75	C32	178.71	
C26	45.83	2.28, 2.37	C43	180.37	
C37	46.51	1.98, 2.44	C50	180.73	
Pr1	47.46	3.26, 3.49	C61	180.73	
C2	49.12		*d*HS		6.52
C12	49.86		*c*HS		6.75
C7	53.31		*d*HA		6.81
C13	55.31	3.18	*e*HS		6.85
C8	57.93	3.60	*b*HS		6.94
C3	58.18	4.11	*a*HS		7.09

Group	δ ^{13}C (ppm)	δ ^{1}H (ppm)	Group	δ ^{13}C (ppm)	δ ^{1}H (ppm)
C17	61.22		*g*HS		7.13
R5	63.55	3.79, 3.89	*e*HA		7.52
R2	72.91	4.50	*c*HA		7.57
Pr2	75.33[d]	4.35	*b*HA		7.66
R3	76.46	4.77	*a*HA		7.84
C19	77.27	4.12	*g*HA		7.99
R4	85.40	4.32	*f* H		8.05
C1	88.24				

[a] In 0.15 M phosphate buffer, pH 7.70, 90% H_2O/10% D_2O, 25 °C. Chemical shifts are relative to internal TSP. The *syn* and *anti* amide H's are designated *a*H_S, *a*H_A, *b*H_S, *b*H_A, *etc.*, respectively, where *a*, *b*, *etc.*, refer to the standard side chain lettering.

[b] $^3J_{PC}$ = 4.2 Hz.

[c] $J_{Pr2\text{-}Pr3}$ = 6.1 Hz.

[d] $^2J_{PC}$ = 5.4 Hz.

[e] $J_{R1,R2}$ = 3.2 Hz.

Table 2

Comparison of ^{13}C NMR chemical shifts for NOCbl, NO_2Cbl and NH_3Cbl[37a]

Group	δ NOCbl	δ NO_2Cbl	(Δδ)	$^{\delta}NH_3Cbl$	(Δδ)
C54	20.34	18.31	(2.03)	19.16	(1.18)
C20	24.48	22.45	(2.00)	22.73	(1.75)
C49	36.04	37.33	(−1.29)	37.36	(−1.32)
C60	37.86	34.05	(3.81)	34.01	(3.85)
C37	46.51	44.80	(1.71)	48.09	(−1.58)
R2	72.91	71.29	(1.62)	71.28	(1.63)
R1	88.51	89.64	(−1.13)	89.77	(−1.26)
C15	107.60	106.05	(1.55)	106.41	(1.19)
B4	121.29	119.07	(2.22)	118.81	(2.48)
B5	133.99	135.64	(−1.65)	135.88	(−1.89)
B8	134.21	132.05	(2.16)	132.09	(2.12)
B6	135.75	137.80	(−2.05)	138.07	(−2.32)
B9	142.20	139.17	(3.03)	139.11	(3.09)
C14	166.30	167.96	(−1.66)	168.23	(−1.93)
C9	174.53	175.89	(−1.36)	177.01	(−2.48)
C16	178.23	180.73	(−2.50)	182.50	(−4.27)
C4	178.71	182.47	(−3.76)	183.73	(−5.02)
C32	178.71	180.44	(−1.73)	180.42	(−1.71)
C61	180.73	178.23	(2.50)	177.63	(3.10)

[a]Only chemical shifts which differ by ≥1.00 ppm from those for NOCbl are shown.

Table 3

Comparison of the DMB ^{13}C NMR Chemical Shifts for NOCbl with those of other XCbl[61,77,78]

Carbon	AdoCbl	CH_3Cbl	CNCbl	H_2OCbl^+	NOCbl	$(CN)_2Cbl^-$	α-AdoCbl
B7	113.14	113.12	114.04	114.50	113.43	113.63	113.89
B4	120.98	120.83	119.00	118.00	121.29	121.59	121.38
B8	133.03	133.06	132.49	131.82	134.21	134.15	134.29
B5	136.27	136.28	135.60	136.41	133.99	135.07	135.91
B6	136.40	136.37	137.67	137.52	135.75	135.92	135.09
B9	140.62	140.75	139.25	138.70	142.20	142.96	142.40
B2	144.20	144.40	144.39	144.70	144.53	145.22	145.20
K_{Co} [a]	76.6	467	2.88×10^5	4.90×10^7		0[b]	0[b]

[a] K_{Co} is the equilibrium constant for formation of the base-on species from the base-off, DMB unprotonated species (Scheme 1).[61]

[b] These Cbls are completely base-off.

Table 4

Estimates of K_{Co} and $pK_{base\text{-}off}$ for NOCbl from the DMB ^{13}C NMR chemical shifts[a]

	Correlation			Calculated for NOCbl		
Carbon	**Slope (ppm kcal^{-1})**	**Intercept (ppm)**	**r^2**	**ΔG_{Co}^{o} (kcal mol^{-1})**	**K_{Co}**	**$pK_{base\text{-}off}$**
B4	0.380 ± 0.025	122.10 ± 0.14	0.966	−2.14	37.1	3.98
B5	−0.306 ± 0.016	133.087 ± 0.084	0.980	−2.17	39.0	3.96
B6	−0.282 ± 0.014	135.437 ± 0.076	0.981	−1.11	6.56	4.68
B8	0.151 ± 0.010	133.420 ± 0.055	0.966	5.22	1.49×10^{-4}	5.56
B9	0.277 ± 0.020	141.64 ± 0.11	0.960	2.67	1.10×10^{-2}	5.56

[a] See Ref. 61 and 62.